

Two-stage coarsening mechanism in a kinetically constrained model of an attractive colloid

Stephen Whitelam¹ and Phillip L. Geissler^{1,2}

¹ Department of Chemistry, University of California,
and Physical Biosciences Division ²and Materials Sciences Division,
Lawrence Berkeley National Laboratory, Berkeley, CA 94720

(Dated: February 26, 2019)

We study an attractive version of the East model using the real-space renormalization group (RG) introduced by Stella et al. The former is a kinetically constrained model with an Ising-like interaction between excitations, and shows striking agreement with the phenomenology of attractive colloidal systems. We find that the RG predicts *two* nonuniversal dynamic exponents, which suggests that in the out-of-equilibrium regime the model coarsens via a two-stage mechanism. We explain this mechanism physically, and verify this prediction numerically. In addition, we find that the characteristic relaxation time of the model is a non-monotonic function of attraction strength, again in agreement with numerical results.

I. INTRODUCTION

In this paper we study the attractive East model introduced by Geissler and Reichman [1], a kinetically constrained model designed to capture the physics of colloidal suspensions with short-ranged attractions [2]. Kinetically constrained models (KCMs) [3, 4, 5, 6] are systems in which certain trajectories between configurations are suppressed [7]. As a result, they possess interesting slow dynamics [8, 9, 10, 11, 12, 13, 14]. Simple KCMs, such as the facilitated spin models introduced by Fredrickson and Andersen [3] (hereafter the FA model) and Jäckle and Eisinger [5] (hereafter the East model) display the slow, cooperative relaxation characteristic of supercooled liquids near the glass transition [13, 14]. For a review of the glassy dynamics of KCMs see [15].

The attractive East model possesses in addition to a kinetic constraint a static attraction between facilitating excitations. It was shown numerically [1] that this model captures some key features of the phenomenology of attractive colloids, such as a re-entrant (non-monotonic) timescale associated with relaxation in equilibrium, and logarithmic relaxation near re-entrance [2].

In this paper we study the attractive East model using the real-space RG scheme of References [20, 21]. Our reasons for doing so are twofold. First, we wish to predict analytically the nature of the model's out-of-equilibrium coarsening behaviour, which we expect to caricature an experiment on a real colloid in which the attraction strength remains fixed but a pressure change induces a change in the equilibrium free volume of the system. The equilibrium behaviour of the attractive East model, modelling a set of experiments in which free volume remains fixed but attraction strength varies, was explored in Reference [1]. Second, we wish to test the utility of the real-space RG scheme, which has previously been applied to quantum spin systems [21], reaction-diffusion systems [20] and simple kinetically constrained models [18].

Our key results, which we present in Section VI, are

as follows. We show that the RG scheme predicts *two* nonuniversal dynamic exponents (by nonuniversal we mean depending on the model's parameters) which suggests that in the out-of-equilibrium regime the model coarsens via a two-stage mechanism. On short wavelengths, relaxation is approximately diffusive; on longer wavelengths, relaxation is dramatically sub-diffusive. We explain this mechanism in terms of a competition between the static attraction and the kinetic constraint, and verify this prediction numerically, as illustrated in Figure 3. In addition, we find that the characteristic relaxation time of the model is a non-monotonic function of attraction strength, in agreement with the numerical results of Ref [1].

This paper is organised as follows. In Section II we define the attractive East model, and for convenience cast its evolution operator in a quantum spin formalism. In Section III we explain the RG scheme of References [20, 21]. In Section IV we apply this RG to the ordinary East model, emphasising the physical interpretation of the scheme, and in Section V we do the same to its attractive counterpart. We thus demonstrate that the formalism can, with little modification, treat both models. Those readers interested principally in the results of our study should focus on Section VI, in which we present our findings, summarised above. We conclude in Section VII.

II. THE MODEL

The attractive East model introduced in Reference [1] is a chain of N binary occupancies $n_i = 0, 1$ with periodic boundary conditions, an interacting reduced Hamiltonian

$$\mathcal{H} = -\epsilon \sum_{i=1}^N n_i n_{i+1} + h(\epsilon, c) \sum_{i=1}^N n_i, \quad (1)$$

where $\epsilon > 0$, and the kinetic constraint of the East model [5]. This constraint dictates that a cell i may

change state only if it possesses a left neighbour in the excited state ($n_{i-1} = 1$). We consider these occupancies to represent immobile ($n_i = 0$) or mobile ($n_i = 1$) regions of the colloid, defined over a suitable microscopic coarse-graining time [1, 13]. We define the equilibrium concentration of mobile regions as c , and we shall refer to occupancies $n_i = 1$ as ‘excitations’.

The attraction ϵ induces correlations between excitations. It should not be taken to represent a literal attraction between mobile regions of a real colloid, but instead to describe the tendency of colloidal *particles* to attract one another [16]. These attractions may be mediated by dissolving a polymer in the colloid, or by changing the concentration of a dissolved salt solution. We regard the field $h(\epsilon, c)$ as an auxiliary variable that depends on c and ϵ in such a way that c is unchanged by varying ϵ : in other words, varying the strength of the inter-molecular attraction does not change the system’s free volume. The required adjustment of field with attraction strength follows from the standard result for the magnetization of an Ising model in $d = 1$ [17],

$$h(\epsilon, c) = \epsilon + 2 \sinh^{-1} \left(\frac{1-2c}{2\sqrt{c(1-c)}} e^{-\epsilon/2} \right). \quad (2)$$

The dynamics of the model is governed by a master equation

$$\partial_t P(n, t) = - \sum_i w(n_i) P(n, t) + \sum_i w(1 - n_i) P(n', t), \quad (3)$$

where $P(n, t)$ is the probability that the system has configuration $n \equiv \{n_1, \dots, n_i, \dots, n_N\}$ at time t (n' is the configuration n with occupancy $n_i \rightarrow 1 - n_i$), and $w(n_i) \equiv w(n_i, \{n_j\})$ is the probability per unit time that n_i will change state. The $\{n_j\}$ are the nearest neighbours of i .

We now pass to a quantum formalism [19] in the manner described in [18]. Equation (3) is recast as the Euclidean Schrödinger equation

$$\partial_t |\Psi(n, t)\rangle = - \sum_i \mathcal{L}_i |\Psi(n, t)\rangle, \quad (4)$$

where the Liouvillian \mathcal{L}_i is

$$\mathcal{L}_i = \mathcal{C}_i(\{s_j\}) \left\{ e^{-\frac{1}{2}(\mathcal{H}(n') - \mathcal{H}(n))} - e^{-\frac{1}{2}(\mathcal{H}(n) - \mathcal{H}(n'))} \hat{\sigma}_i \right\}. \quad (5)$$

The state vector $|\Psi(n, t)\rangle$ is a tensor product of single-site state vectors,

$$|\Psi(n, t)\rangle = \sum_{\{n\}} P(n, t) \prod_{i=1}^N \otimes |n_i\rangle, \quad (6)$$

and $\hat{\sigma}_i$ is the spin-flip operator, defined via $\hat{\sigma}_i f(n) \equiv f(n') \hat{\sigma}_i$. The kinetic constraint is $\mathcal{C}_i(\{n_j\}) = n_{i-1}$, and so suppresses the dynamics of cell i if cell $i-1$ is unexcited.

We can write the Liouvillian (5) as [18]

$$\begin{aligned} \mathcal{L}_i = & 1_1 \otimes \cdots \otimes n_{i-1} \otimes \ell_{i,(2)} \otimes n_{i+1} \otimes 1_{i+2} \otimes \cdots \otimes 1_N \\ & + 1_1 \otimes \cdots \otimes n_{i-1} \otimes \ell_{i,(1)} \otimes v_{i+1} \otimes 1_{i+2} \otimes \cdots \otimes 1_N, \end{aligned} \quad (7)$$

where $v_i \equiv 1 - n_i$ is the vacancy operator. The full Liouvillian is composed of a sum of terms like those in (7), with one factor for each site of the lattice. All factors in (7) are 2×2 matrices.

We can write the Liouvillian schematically as

$$\mathcal{L} = n \otimes \ell_2 \otimes n + n \otimes \ell_1 \otimes v, \quad (8)$$

where we have dropped site labels for brevity. Using the representation

$$\hat{\sigma}_i = \begin{pmatrix} 0 & 1 \\ 1 & 0 \end{pmatrix}, \quad n_i = \begin{pmatrix} 1 & 0 \\ 0 & 0 \end{pmatrix}, \quad (9)$$

we can write the single-site Liouvillians as

$$\ell_k \equiv \begin{pmatrix} e^{h/2-k\epsilon/2} & -e^{-h/2+k\epsilon/2} \\ -e^{h/2-k\epsilon/2} & e^{-h/2+k\epsilon/2} \end{pmatrix}, \quad (10)$$

where the excitation number $k = 1, 2$. The off-diagonal elements of ℓ_k control the rates for the flipping processes: if n_i has two neighbouring excitations ($k = 2$) it will excite with rate $e^{-h/2+\epsilon}$, and de-excite with rate $e^{h/2-\epsilon}$ [note the global minus sign in Equation (4)]. If only its left neighbour is excited ($k = 1$), n_i will excite with rate $e^{-h/2+\epsilon/2}$ and de-excite with rate $e^{h/2-\epsilon/2}$. Since $h-\epsilon$ is a monotonically decreasing function of ϵ [1], the attraction ϵ encourages excitations to congregate.

The diagonal elements of ℓ_k are such that the sum of elements in each column is zero, a property that is required by any probability-conserving stochastic process. We shall call this property *stochasticity* [20], and we shall require that it be preserved under renormalization.

III. REAL-SPACE RENORMALIZATION GROUP

We shall study the attractive East model using a real-space RG developed in the 1980s, previously applied to quantum spin models [21] and reaction-diffusion systems [20]. The procedure is as follows. First, one partitions the lattice into blocks of b spins; we shall take $b = 2$. Then one splits the Liouvillian \mathcal{L} into a reference, intra-block piece \mathcal{L}_0 , and an inter-block interaction V in which an expansion will be made. By performing a suitable coarse-graining from the original lattice to a renormalized block-spin lattice, one obtains a coarse-grained or renormalized Liouvillian from which one may infer the scaling properties for the model in question. In Ref. [18] we showed that this scheme yields the low-temperature critical behaviour of some simple kinetically constrained models in one dimension.

Because the attractive East model possesses 3-site interaction terms we must go to $\mathcal{O}(V^2)$ in the perturbation

expansion. We shall outline the procedure; see [21] for more details.

We first split the Liouvillian into a reference piece and a perturbation,

$$\mathcal{L} = \mathcal{L}_0 + \eta V, \quad (11)$$

where η is a parameter we shall use to organise the perturbation expansion. The reference piece \mathcal{L}_0 consists only of intra-block operators, whereas the interaction V includes inter-block interactions. For example, \mathcal{L}_0 might look like

$$\mathcal{L}_0 = (n \otimes \ell) \otimes (1 \otimes 1), \quad (12)$$

where the brackets indicate the way in which we choose to partition sites into renormalized cells. The inter-block interaction V might then look like

$$V = (1 \otimes n) \otimes (\ell \otimes 1), \quad (13)$$

where now the nontrivial operators n and ℓ are split between the notional renormalized cells.

Next, we introduce the right eigenstates $|\phi_i\rangle = \{|g_j\rangle, |e_l\rangle\}$ of the reference Liouvillian,

$$\mathcal{L}_0 |\phi_i\rangle = E_{\phi_i} |\phi_i\rangle, \quad (14)$$

where $|\phi_i\rangle$ includes both ground states $|g_j\rangle$ with $E_{g_j} = 0$, and excited states $|e_l\rangle$ with $E_{e_l} \neq 0$. We shall find that the reference state we choose for the attractive East model has three ground states ($j = 1, 2, 3$) and one excited state ($l = 1$). Ground states describe slow processes, and excited states describe fast processes.

We require also the left eigenstates of the reference Liouvillian,

$$\langle \phi_i | \mathcal{L}_0 = \langle \phi_i | E_{\phi_i}, \quad (15)$$

which are generally distinct from the right eigenstates for non-Hermitian Liouvillians.

The renormalization prescription is defined by a relationship between the renormalized Liouvillian \mathcal{L}' and its unrenormalized counterpart \mathcal{L} :

$$e^{-\mathcal{L}'t'} = \text{Tr } e^{-\mathcal{L}t}. \quad (16)$$

Here $t' \equiv b^{-z}t$ is a renormalized time, and the trace on the right hand side of Equation (16) is taken over excited states, encoding fast processes. What remains should be an evolution operator for slow, coarse-grained dynamical processes.

To evaluate Equation (16) we shall expand the Liouvillian in powers of ηV [22]. The formal solution to (4) is

$$|\Psi(n, t)\rangle = e^{-\mathcal{L}t} |\Psi(n, 0)\rangle. \quad (17)$$

We shall assume that at long times the probability of finding the system in a given configuration is dominated by the reference Liouvillian, i.e.

$$|\Psi(n, t)\rangle \approx e^{-\mathcal{L}_0 t} |\Psi(n, 0)\rangle. \quad (18)$$

Note that this assumption constitutes an uncontrolled approximation. If (18) holds, then $e^{\mathcal{L}_0 t} |\Psi(n, t)\rangle$ varies slowly with time, and so

$$\partial_t (e^{\mathcal{L}_0 t} |\Psi(n, t)\rangle) = \eta e^{\mathcal{L}_0 t} V |\Psi(n, t)\rangle \quad (19)$$

is small. Integrating Equation (19) with respect to time gives us a self-consistent equation for the configuration probability $|\Psi(n, t)\rangle$,

$$|\Psi(n, t)\rangle = e^{-\mathcal{L}_0 t} |\Psi(n, 0)\rangle - \eta \int_0^t dt' e^{\mathcal{L}_0(t'-t)} V |\Psi(n, t')\rangle. \quad (20)$$

The first term in (20) is our ansatz for the long-time state of the system, and the second term is a perturbation, assumed small. Expanding (20) to second order in ηV , and invoking the arbitrary nature of $|\Psi(n, t)\rangle$ allows us to infer the operator equation

$$e^{-\mathcal{L}t} \approx e^{-\mathcal{L}_0 t} - \eta t e^{-\mathcal{L}_0 t} V + \eta^2 e^{-\mathcal{L}_0 t} \int_0^t dt' V(t') \int_0^{t'} dt'' V(t''), \quad (21)$$

where $V(t) \equiv e^{\mathcal{L}_0 t} V e^{-\mathcal{L}_0 t}$. We next insert (21) into (16), and trace over excited states. We further assume that the renormalized Liouvillian \mathcal{L}' can be expanded in powers of η :

$$\mathcal{L}' = \mathcal{L}'_0 + \eta \mathcal{L}'_1 + \eta^2 \mathcal{L}'_2 + \dots \quad (22)$$

If we expand both sides of (16) to $\mathcal{O}(\eta^2)$ and equate powers of η , we get

$$\mathcal{L}'_0 = 0; \quad (23)$$

$$\mathcal{L}'_1 = \langle g_i | V | g_j \rangle; \quad (24)$$

$$\mathcal{L}'_2 = - \sum_k \langle g_i | V | e_k \rangle \frac{1}{E_{e_k}} \langle e_k | V | g_j \rangle, \quad (25)$$

where we have suppressed terms sub-leading in t , justified at large t . The second order result (25) is required only if the Liouvillian of the model under study possesses n -site interaction terms, with $n > 2$, as is the case for the attractive East model. For the ordinary East model, which contains only two-site interactions, the first order term (24) is sufficient.

The factor of $E_{e_k}^{-1}$ in (25) weights the relative contributions of excited states to the renormalization procedure. States with small eigenvalues, those corresponding to slower processes, are accorded more importance as a consequence of this factor.

The excited states $|e_i\rangle$ divide into two classes: those containing single-cell excitations, and those containing two-cell excitations. Higher-order contributions vanish by virtue of the relation $\langle g_i | e_j \rangle = 0$, and the fact that the model we study contains at most three-site, or two-cell interactions. We thus write

$$|e_i\rangle = |e_i^I\rangle + |e_i^{II}\rangle, \quad (26)$$

where

$$|e_i^I\rangle = \sum_{k=1}^{\alpha} \sum_{j=1}^N |g_k\rangle_1 \otimes \cdots \otimes |e_i\rangle_j \otimes |g_k\rangle_{j+1} \otimes \cdots \otimes |g_k\rangle_N, \quad (27)$$

and

$$|e_i^{II}\rangle = \sum_{k=1}^{\alpha} \sum_{j=1}^N |g_k\rangle_1 \otimes \cdots \otimes |e_i\rangle_j \otimes |e_i\rangle_{j+1} \otimes |g_k\rangle_{j+2} \otimes \cdots \otimes |g_k\rangle_N \quad (28)$$

Note that α denotes the number of ground states, equal to 3 for the model we shall study. We impose the normalization $\langle g_i | g_j \rangle = \delta_{ij} = \langle e_i | e_j \rangle$.

In the following section we describe how this formalism may be used to treat the ordinary East model, emphasising the physical interpretation of the procedure. In section V we apply this formalism to the attractive East model.

IV. RG FOR THE EAST MODEL

In this section we shall outline the application of the RG procedure described above to the East model [18]. We show that it is possible to define the scheme by imposing normalization and probability conservation, together with knowledge of the peculiar hierarchical dynamics of the East model. This allows us to show that the RG for the attractive East model, which we discuss in the following section, can be determined by straightforward generalization of the result for its noninteracting counterpart.

The Liouvillian of the East model is

$$\mathcal{L} = n \otimes \ell, \quad (29)$$

where

$$\ell \equiv \begin{pmatrix} 1-c & -c \\ c-1 & c \end{pmatrix}, \quad (30)$$

and $c \approx e^{-1/T}$ is the excitation rate of a facilitated cell. Equation (29) describes the dynamics of a cell facilitated only by a left-neighbouring excitation. The RG prescription (24) may be written

$$\mathcal{L}'(n') = T_1(n', n) \cdot \mathcal{L}(n) \cdot T_2(n, n'), \quad (31)$$

where T_1 and T_2 are respectively $2^{N/2} \times 2^N$ and $2^N \times 2^{N/2}$ -dimensional matrices built from the left (T_1) and right (T_2) ground-state eigenvectors of \mathcal{L}_0 . The RG prescription is thus a mapping from a 2^N -dimensional Hilbert space of ‘real’ occupancies to a $2^{N/2}$ -dimensional Hilbert space of renormalized occupancies, which we distinguish with primes.

As discussed in Ref. [18], we find that T_1 and T_2 have simple interpretations in terms of the dynamics of the model under study. The projection matrix T_1 takes a

‘real’ state $\{11, 10, 01, 00\}$ and projects it onto a renormalized state. For the East model we find that any state with at least one excitation projects onto a renormalized excitation. Thus $T_1 = t_1^{\otimes N/2}$ where

$$t_1 = |1'\rangle \{ \langle 11| + \langle 10| + \langle 01| \} + |0'\rangle \langle 00| \quad (32)$$

Hence blocks of spins which can, within a single time step, facilitate neighbouring spins are deemed also to be facilitating in the coarse-grained sense. Note that if we were to renormalize an Ising model with no kinetic constraint, then we would require that flipping a spin in an unrenormalized configuration would result in the flipping of the coarse-grained spin. This is not the case for kinetically constrained models, for which there is no symmetry between excitations and vacancies.

The embedding matrix T_2 reconstitutes a real state from a coarse-grained state, and in a sense identifies those original states most important for the low temperature dynamics of the system. As discussed in [18], T_2 respects both energetic and entropic effects. For the East model we have $T_2 = t_2^{\otimes N/2}$, where

$$t_2 = \frac{1}{1+\lambda} \{ \lambda |11\rangle + |10\rangle \} \langle 1'| + |00\rangle \langle 0'|. \quad (33)$$

We have defined $\lambda \equiv c/(1-c)$. The structure of (33) is found from the right ground-state eigenvectors of \mathcal{L}_0 , together with the requirements of normalization and conservation of probability [18], but may be simply motivated as follows. To find t_2 , one adds to the term $|00\rangle \langle 0'|$ a sum of terms $(1+\lambda)^{-1} \lambda^{n_1+n_2-1} |n_1, n_2\rangle \langle 1'|$, where $n_1 n_2$ is an unrenormalized configuration, and the power of λ accounts for the energetic weighting of these states. Thus the state 11 is penalized by a factor of λ , whereas the state 10 receives no penalty.

According to this rule we should also include in (33) a term $(1+\lambda)^{-1} |01\rangle \langle 1'|$, but here entropic effects come into play. The East model possesses an hierarchical dynamics [9, 15], whereby two excitations separated by a distance d are relaxed by establishing a set of isolated excitations between them, at distances $d/2, 3d/4$ etc. We can incorporate this behaviour into our RG scheme by suppressing ‘frozen’ configurations 01 during embedding, which is permitted by the structure of the ground state eigenvectors of the East model reference Liouvillian. Under repeated application of this modified embedding operator we then see that the most important state in the dynamical sense for $d=4$ is

$$1011, \quad \text{weight } 1 \times c^2, \quad (34)$$

and not, for instance,

$$1001, \quad \text{weight } 0 \times c. \quad (35)$$

The latter state is favoured thermodynamically over the former, because it contains one fewer excitation, but the latter is suppressed entropically (the factor 0 multiplying

c^2). To see this, note that in order to relax the rightmost excitation in state (35) we must excite the second spin, followed by the third, and then finally we may relax the rightmost spin. To perform a similar relaxation for state (34) we may simply relax the rightmost state. Thus in an approximate sense we see that the peculiar structure of T_2 respects the hierarchical dynamics of the East model. Note that for the FA model, which has symmetrical dynamical rules, no such entropic suppression operates. States (34) and (35) would then be of similar importance to the dynamics.

The renormalization prescription can thus be thought of as a scheme that picks out those dynamical trajectories that most readily relax the system. As detailed in [18] we find for the East model the dynamic exponent $z = 1/(T \ln 2)$, to leading order in T , and a marginally unstable critical point at $T = 0$, at which the recursion relation for the temperature parameter satisfies $\lambda' = \lambda + \lambda^2$. The scaling properties of the East model at low temperature then follow. For example, based on the existence of a critical point we can write down a scaling relation for the density of excitations n in the out-of-equilibrium regime,

$$n(t, \lambda) = e^{-d\ell} \hat{n}(t(\ell), \lambda(\ell)). \quad (36)$$

Here $d = 1$ is the physical dimension, $\ell = \ln b$ parameterizes the lattice rescaling parameter (now taken to be a real number), \hat{n} is a dimensionless scaling function, and the arguments on the right hand side of (36) are the renormalized flowing time $t(\ell) = e^{-z\ell} t$ and temperature parameter $\lambda(\ell) = 1/(\lambda^{-1} - \ln(\ell/\ell_0))$, respectively. Equation (36) relates a real system at long times and low densities (left hand side) to an effective, renormalized system at short times and high densities (right hand side). By imposing the matching condition $e^{-z\ell} t = 1$ we find in the regime $0 \ll \ln t \ll 1/(T^2 \ln 2)$ the anomalous coarsening behaviour

$$n(t) \sim t^{-T \ln 2}, \quad (37)$$

which has been derived by other means and verified numerically [15].

V. RG FOR THE ATTRACTIVE EAST MODEL

We now apply the formalism of Section 2 to the attractive East model, and find that, to first order, the scheme is a straightforward generalization of that of the previous section.

The attractive East model Liouvillian is

$$\mathcal{L} = n \otimes \ell_2 \otimes n + n \otimes \ell_1 \otimes v. \quad (38)$$

In order to obtain a reference Liouvillian that contains only two-site interactions, we write the vacancy operator v in the second term on the right hand side of (38) as $1 - n$, to get

$$\mathcal{L} = n \otimes \ell_1 + n \otimes \Delta \otimes n, \quad (39)$$

where $\Delta \equiv \ell_2 - \ell_1$. We choose as our reference Liouvillian

$$\mathcal{L}_0 = n \otimes \ell_1. \quad (40)$$

The ground state embedding and projection operators are then similar to those for the ordinary East model. The projection operator T_1 is identical, which may be motivated in a physical way by considering that the definition of a facilitating spin in the attractive East model is identical to that in its ordinary counterpart. The embedding operator $T_2 = t_2^{\otimes N/2}$ now accounts for the attraction-modified Boltzmann weights of two-site configurations: the attraction ‘rewards’ neighbouring excitations with an energy $-2e$ with respect to an excitation-vacancy pair. Note that the entropic suppression of the state 01 still operates. We thus find

$$t_2 = \frac{1}{e^{\epsilon-h} + 1} (e^{\epsilon-h} |11\rangle + |10\rangle) \langle 1'| + |00\rangle \langle 0'|, \quad (41)$$

where $h = h(\epsilon, c)$. In the limit $\epsilon \rightarrow 0$ we recover Equation (33), with $\lambda \rightarrow e^{-h}$. For the second order result (25) we require also the excited projection matrix $E_1 = e_1^{\otimes N/2}$ and embedding matrix $E_2 = e_2^{\otimes N/2}$, which are determined by

$$e_1 = |1'\rangle (\langle 10| - e^{-\epsilon+h} \langle 11|), \quad (42)$$

and

$$e_2 = (1 + e^{h-\epsilon})^{-1} (-|11\rangle + |10\rangle) \langle 1'|. \quad (43)$$

The prefactor in (43) ensures that $e_1 \cdot e_2 = 1$.

We now write our Liouvillian as $\mathcal{L} = \mathcal{L}_0 + V$, where

$$\mathcal{L}_0 = (n \otimes \ell_1) \otimes (1 \otimes 1) \quad (44)$$

and

$$V = A \otimes B + C \otimes D, \quad (45)$$

with $A \equiv (1 \otimes n)$, $B \equiv (\ell_1 \otimes 1 + \Delta \otimes n)$, $C \equiv (n \otimes \Delta)$ and $D \equiv (n \otimes 1)$. The brackets denote the blocking of the lattice into cells.

We find under renormalization that to first order

$$\mathcal{L}'_1 = t_1 A t_2 \otimes t_1 B t_2, \quad (46)$$

and to second order

$$\begin{aligned} \mathcal{L}'_2 = & t_1 A e_2 \cdot e_1 A t_2 \otimes t_1 B t_2 \cdot t_1 B t_2 + \\ & t_1 A e_2 \cdot e_1 C t_2 \otimes t_1 B t_2 \cdot t_1 D t_2 + \\ & t_1 A t_2 \cdot t_1 A t_2 \otimes t_1 B e_2 \cdot e_1 B t_2 + \\ & \frac{1}{2} t_1 A e_2 \cdot e_1 A t_2 \otimes t_1 B e_2 \cdot e_1 B t_2 + \\ & t_1 A t_2 \otimes t_1 B e_2 \cdot e_1 C t_2 \otimes t_1 D t_2. \end{aligned} \quad (47)$$

We can make sense of these results by noting that the combination $t_1 A t_2 = n'$ is a renormalized number operator, and $t_1 B t_2 = \ell'$ is a renormalized single-site Liouvillian. Hence the first order result (46) looks like a renormalized (ordinary) East model, $\mathcal{L}' = n' \otimes \ell'$. The second

order 2-site terms, the first four lines of Equation (47), also have the form ‘constraint \otimes rate’, or $n' \otimes \tilde{\ell}'$. Note that the fourth term arises from a two-cell excitation, and so, by virtue of the factor of E_k^{-1} in Equation (25), enters with a factor of $\frac{1}{2}$. The final term in (47) is a three-site interaction that allows us to write \mathcal{L}_2 in the form (8), and so to unambiguously determine the behaviour of the attractive East model under renormalization. We shall do this in the following section.

In addition, to second order, we find two terms corresponding to operators not present in the original Liouvillian, namely

$$\begin{aligned}\tilde{\mathcal{L}}'_2 = & t_1 At_2 \otimes t_1 Ae_2 \cdot e_1 Bt_2 \otimes t_1 Bt_2 + \\ & t_1 At_2 \otimes t_1 Be_2 \cdot e_1 At_2 \otimes t_1 Bt_2.\end{aligned}\quad (48)$$

For example, the second term in (48) represents a non-local facilitation of the form $n'_{i-1} \otimes \dots \otimes \ell'_{i+1}$. Hence to this order the renormalization procedure is not closed. We shall ignore these terms.

VI. RESULTS OF OUR STUDY

With the renormalized Liouvillian now in hand we can extract the scaling properties of the attractive East model in the limit of small defect concentrations and long times. The first order result (46) shows that in the long time- and large length-scale limit the model behaves like an ordinary East model with renormalized parameters. This agrees with the analysis of [1], which concluded that the attractive East model behaves on long length scales as an ordinary East model, albeit with a rescaled typical width of excited domains. We shall use the second order RG result (47) to infer the ‘flow’ of the model towards this ‘renormalized’ East-like behaviour. To extract the dynamic exponent z , however, it is sufficient to use the first-order result, which describes the slowest dynamically relevant processes. We proceed as follows.

The dynamic exponent z , defined via $t' = b^{-z}t$, describes the rescaling of time as a consequence of rescaling space by a factor of b^{-1} . Hence we can determine z by studying the ratio of renormalized to unrenormalized rates. We define the rates Γ_α , $\alpha \in \{1, 2, 3, 4\}$, for the four processes of the model as follows:

α	Process	Γ_α
1	$111 \rightarrow 101$	$e^{h/2-\epsilon}$
2	$110 \rightarrow 100$	$e^{h/2-\epsilon/2}$
3	$101 \rightarrow 111$	$e^{-h/2+\epsilon}$
4	$100 \rightarrow 110$	$e^{-h/2+\epsilon/2}$

Let us define the renormalized rates $\Gamma_\alpha^{(1)}$ extracted from the first order result (46). Then upon rearranging $\Gamma^{(1)} = b^{-z}\Gamma$ we have $z_\alpha = -\ln r_\alpha / \ln 2$, where $r_\alpha \equiv \Gamma_\alpha^{(1)} / \Gamma_\alpha$. The renormalized rates are cumbersome, and so we shall not display them explicitly.

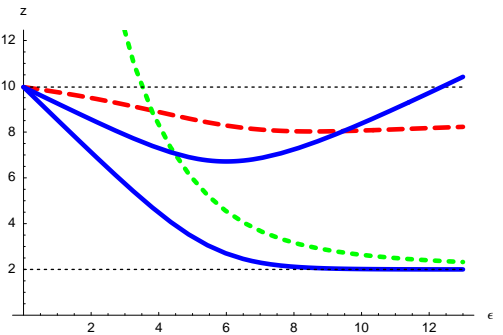


FIG. 1: Dynamic exponent z versus attraction strength ϵ for the attractive East model, at excitation concentration $c = 10^{-3}$. The lower horizontal line marks the diffusive limit $z = 2$; the upper horizontal line is the prediction for the East model in the absence of the attraction. The bold dashed lines are the phenomenological predictions z_2 (lower line, green) and z_3 (upper line, red). These we expect to be characteristic values for the dynamic exponent of the attractive East model when the domain sizes are respectively much less than and much greater than the attraction-induced lengthscale $a(\epsilon, c)$. The bold blue lines are the prediction for z from the first-order RG calculation. Both correctly reproduce the $\epsilon \rightarrow 0$ limit, and agree with our numerical results (see Figure 3).

We find that, unlike for the ordinary East model, there is no common rescaling factor z . Instead we find four distinct z_α , whose dependence upon ϵ is dramatically different. Two values, z_1 and z_4 , we discard as unphysical, being negative and tending asymptotically to unity, respectively. The other two we plot for excitation concentration $c = 10^{-3}$ in Figure 1. The larger value, z_3 , is non-monotonic, and follows approximately the behaviour of the East-like exponent. The smaller value, z_2 , tends to a diffusive value 2 for large attraction strengths.

We can understand the nature of these two dynamic exponents from the following simple argument. The dynamic exponent characterizes the typical rate τ^{-1} at which a domain wall can move a given distance ℓ , via $\tau \sim \ell^z$. Let us define a diffusion constant D , such that

$$\ell^2 \equiv \langle (r(\tau) - r(0))^2 \rangle = 2D\tau, \quad (49)$$

and $r(\tau)$ is the position of a given domain wall at time τ . Replacing the exponent 2 in Equation (49) by the more general value z , we can write

$$\tau \sim D^{-1} \ell^z. \quad (50)$$

But if we consider domain wall drift as an ‘activated’ process, one inhibited by an effective energy barrier of size $\Delta(\ell)$, then we can also write

$$\tau \sim \Gamma_0^{-1} \exp(\Delta(\ell)/T), \quad (51)$$

where $\Gamma_0 \sim D$ is the rate for attempting a barrier crossing. Equating (50) and (51) and taking logarithms gives

$$z \sim \frac{\Delta(\ell)/T}{\ln \ell}. \quad (52)$$

Note that the effective barrier $\Delta(\ell)$ accounts for the dynamics of the process under consideration. For example, for the ordinary East model the barrier $\Delta(\ell)/T \approx \ln \ell / \ln 2$ grows logarithmically with ℓ [9], and so we recover $z \sim 1/(T \ln 2)$ to leading order in T .

The two dynamic exponents we find in the case of the attractive East model arise because the attraction imposes a length scale below which the East-like hierarchical dynamics is suppressed. This follows from the fact that there exists in the attractive East model a characteristic width $a(c, \epsilon)$ of excited (black) domains [1]. To see this, note that the energy of a configuration $10 \cdots 01$ of length a is $2h$. The energy of a similar length of chain with all the intermediate cells excited is $h + a(h - \epsilon)$. These energies are equal when $a = h/(h - \epsilon)$. Hence a , which increases as ϵ increases, sets a length scale below which a 10 domain wall can readily move eastwards via a mechanism that excites contiguous cells. See Figure 2 for an illustration of this effect. This domain wall cannot move freely, however; the penalty for exciting successive cells to the east is, from (1), $h - \epsilon$. Thus domain wall motion on lengthscales $\ell \leq a$ should proceed principally by diffusion in a potential $(h - \epsilon)\ell$. The largest barrier to be surmounted is therefore $(h - \epsilon)a$, and so

$$z_2 \sim \frac{(h - \epsilon)a}{\ln a}. \quad (53)$$

We call this exponent z_2 as per the RG notation, and we expect it to dictate the dynamics of the system when the characteristic domain size $L(t)$ satisfies $L(t) \leq a$.

However, on lengthscales $L(t) > a$ we expect relaxation to proceed via East-like hierarchical dynamics, suitably rescaled to account for the attraction-induced length a . A characteristic value for the relevant dynamic exponent can be derived by considering the typical size of white domains in thermal equilibrium, $\langle L(t \rightarrow \infty) \rangle = d(c, \epsilon)$. This length may be found by taking a partial trace over the partition function of the $d = 1$ Ising model. Denoting by λ the largest eigenvalue of the transfer matrix

$$T_{n_i, n_{i+1}} = \begin{pmatrix} 1 & e^{h/2} \\ e^{h/2} & e^{h-\epsilon} \end{pmatrix}, \quad (54)$$

we have that white domains of size L occur with probability $P(L) = \exp(-L \ln \lambda)$. Hence the typical white domain size in equilibrium is $d(c, \epsilon) = 1/\ln \lambda$.

The logarithmic barrier confronting domain walls moving a distance $d \gg a$ is then $\Delta(d)/T = h \ln(d/a)/\ln 2$ [1], and so

$$z_3 \sim \frac{h \ln(d/a)}{\ln d \ln 2}. \quad (55)$$

We show in Figure 1 the dynamic exponents calculated from both phenomenological and RG predictions. In Figure 3 we show numerical results for the attractive East model in the nonequilibrium regime. The coarsening mechanism is as we predict from RG and physical considerations: approximately diffusive relaxation on short

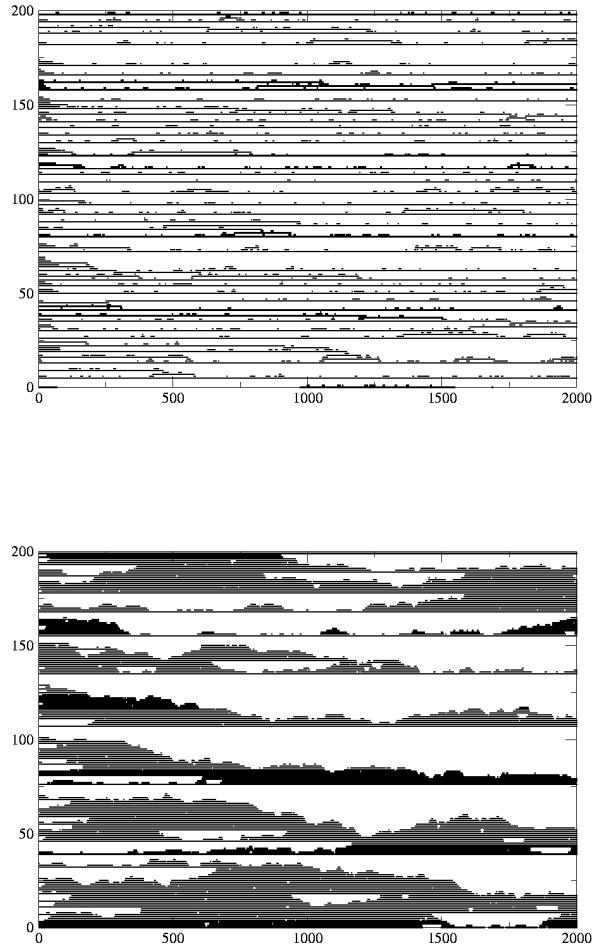


FIG. 2: An illustration of the finite thickness of excited (black) domain walls induced by the attraction ϵ . We show here nonequilibrium space-time trajectories for the attractive East model, starting from excitation concentration $n(0) = 0.5$ for equilibrium excitation concentration $c = 0.1$. We show the cases $\epsilon = 0$ (upper panel) and $\epsilon = 5$ (lower panel). Space runs along the vertical axis, time along the horizontal. Notice the emergence of a finite thickness of excited domains in the lower plot, for which the attraction-induced lengthscale $a \approx 24$ lattice sites. On lengthscales $\ell \leq a$ we expect essentially diffusive dynamics.

wavelengths, crossing over to dramatically sub-diffusive behaviour on larger wavelengths. The crossover length (the position of the ‘kink’ in the plots) is consistent with $\ell(t) \sim a$. For large values of ϵ the distribution of white bubble lengths is very broad, and the crossover begins while the mean domain length is still appreciably less than a .

We verified also that diffusive coarsening persists

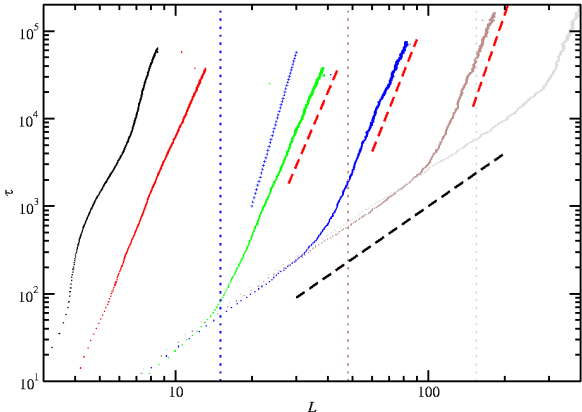


FIG. 3: Continuous time Monte Carlo simulation data for the attractive East model with $c = 10^{-3}$, showing elapsed time τ (vertical axis) versus mean white domain length L (horizontal axis). The system size is $N = 10^5$. We show the average of 10 runs for each attraction strength $\epsilon = 0, 2, 6, 8, 10, 12$, from left to right. The two-stage coarsening mechanism is seen clearly in the three curves at largest ϵ , and the crossover occurs when the mean domain length exceeds approximately $a(c, \epsilon)$. Note that the domain length distribution broadens as the model slows, and so the mean domain length becomes progressively less good as an estimate of the crossover. We show the value of a as vertical dotted lines for $\epsilon = 8, 10$ and 12 . We show also the RG predictions for short-wavelength coarsening at large ϵ , $z = 2$ (heavy black dashed line), and for long-wavelength coarsening for $\epsilon = 6$ ($z \approx 6.72$), $\epsilon = 8$ ($z \approx 7.24$) and $\epsilon = 10$ ($z \approx 8.37$) (heavy red dashed lines). We show for comparison next to the $\epsilon = 6$ line the ordinary East model prediction $z \approx 9.97$ (thin blue line), which clearly disagrees with the data.

throughout the nonequilibrium regime for systems such that $a > d$.

In addition to the dynamic exponent, we can infer from the RG a characteristic timescale for relaxation, and a characteristic length for crossover from diffusive to subdiffusive relaxation. We proceed as follows.

We infer the values of the renormalized parameters via the matrix elements of the renormalized Liouvillian to second order, $\mathcal{L}' = \mathcal{L}'_1 + \mathcal{L}'_2$. In particular, we define the quantities

$$\alpha^{(2)} \equiv \frac{\Gamma_3^{(2)}}{\Gamma_1^{(2)}}; \quad \beta^{(2)} \equiv \frac{\Gamma_1^{(2)} \Gamma_4^{(2)}}{\Gamma_3^{(2)} \Gamma_2^{(2)}}, \quad (56)$$

whose unrenormalized counterparts are $\alpha = e^{2\epsilon - h(c, \epsilon)}$ and $\beta = e^{-\epsilon}$. From the latter two expressions we solve for c and ϵ as functions of α and β , obtaining $c = f(\alpha, \beta)$ and $\epsilon = -\ln \beta$. The function f is unwieldy, by virtue of the complicated dependence of $h(c, \epsilon)$ upon its ar-

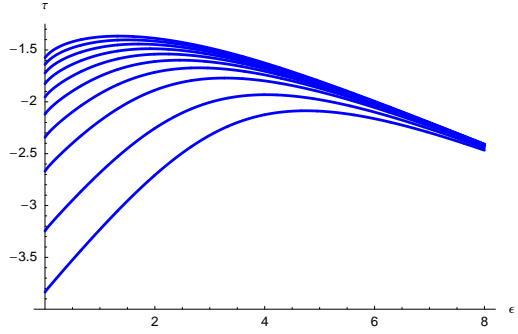


FIG. 4: Negative of the logarithm of the characteristic timescale $-\log_{10} \tau = \nu_{\parallel} \log_{10} c$ from the second-order RG result, for $c = 0.01, 0.02, 0.04, 0.06, 0.08, 0.10, 0.12, 0.14, 0.16, 0.18$ (bottom to top). The degree of non-monotonicity at each value of c is in good agreement with the numerical results shown in Figure 3 of Reference [1]. The difference in absolute value at each concentration occurs because the RG result refers to a generic timescale τ . For any given process τ_g there exists a basic rate $\Gamma(c, \epsilon)$ such that $\tau_g = \Gamma(c, \epsilon) c^{-\nu_{\parallel}}$, and hence the vertical offset of $-\log_{10} \tau_g$ relative to the generic value $-\log_{10} \tau_g$ is $-\log \Gamma(c, \epsilon)$.

guments, Equation (2), and so we shall not display it explicitly. Then we define renormalized parameters via $c' \equiv c^{(2)} = f(\alpha^{(2)}, \beta^{(2)})$ and $\epsilon' \equiv \epsilon^{(2)} = -\ln \beta^{(2)}$.

In the absence of attraction the recursion relation for c under renormalization reads $c = c/(1 - c + c^2)$, encoding an unstable critical fixed point $c^* = 0$ and a stable full-lattice fixed point $c^* = 1$. We shall focus on the the regime $c \ll 1$, and shall avoid probing the large- ϵ regime where possible static critical effects intrude.

To extract a characteristic timescale we define the exponent y_c via $c' = b^{y_c} c$. From standard RG arguments [28] we then have that $\nu_{\perp} = 1/y_c$, where ν_{\perp} controls the divergence of the correlation length ξ near the critical point $c = 0$, via $\xi \sim c^{-\nu_{\perp}}$. Scaling arguments [26] dictate that the characteristic timescale diverges near $c = 0$ as $\tau \sim c^{-\nu_{\parallel}}$, where $\nu_{\parallel} = z\nu_{\perp}$. We plot the logarithm of this timescale, $\log_{10} \tau = \nu_{\parallel} \log_{10} c$, in Figure 4. We find a similar degree of non-monotonic behaviour (roughly 1 decade at the lowest concentrations c) to that shown in Figure 3 of Reference [1]. For consistency we use the exponent z_3 calculated to second order. We expect this exponent to be relevant on large wavelengths, for example in equilibrium for $d \gg a$, as was the case for those simulations shown in Figure 3 of Reference [1].

Lastly, we can infer the lengthscale at which the attractive East model crosses over from near-diffusive to subdiffusive behaviour. To extract such a crossover length, recall that the first order RG result, Equation (24), looks like the Liouvillian of an ordinary East model (with rescaled parameters), in that the rates for excitation and relaxation of a cell are unaffected by the state of the

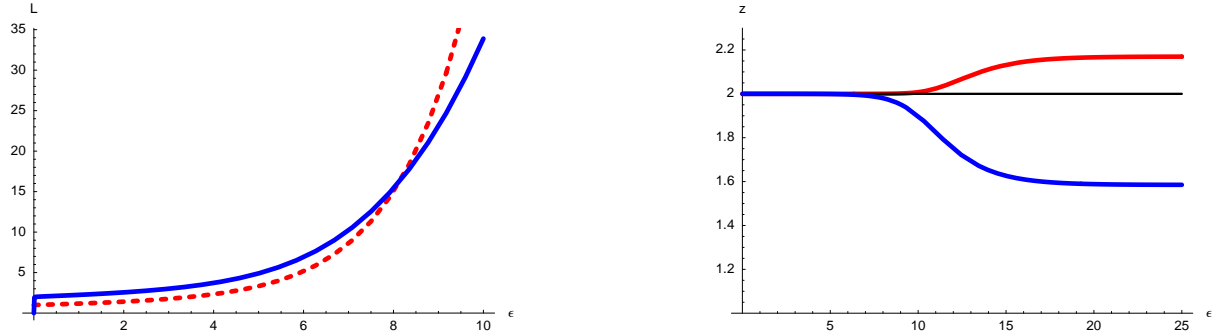


FIG. 5: Crossover length $L_{xo} = (\epsilon_s/\epsilon)^{1/y_\epsilon}$ calculated from the second-order RG result, for $c = 10^{-3}$, as a function of ϵ (solid blue line). We show also the phenomenological prediction $a(c = 10^{-3}, \epsilon)$ (red dashed line). The RG result gives correctly the trend of increasing crossover length with increasing ϵ , as we expect on physical grounds. However, additional physical input is needed to fix the absolute scale of the crossover. Here we obtain close agreement between the two curves by choosing arbitrarily $\epsilon_s = 10^{-3}$, but the RG result varies strongly with ϵ_s and can be made to look very different from $a(c, \epsilon)$.

neighbour to the east. By contrast, the original Liouvillian (8) and the second order RG result (25) describe models whose dynamics depends on the state of a cell's east neighbour.

We thus identify the parameter β in Equation (56) as a measure of the extent to which the model looks 'East-like' (rates insensitive to the state of the east neighbour) or 'attractive East-like' (rates dependent upon the state of the east neighbour). We equate the former situation with the regime of hierarchical (dramatically sub-diffusive) coarsening.

In the language of RG, then, we expect sub-diffusive behaviour when the renormalized parameter ϵ' becomes small. Let us define the exponent y_ϵ via $\epsilon' \sim b^{-y_\epsilon} \epsilon$. From the linearized second-order result we find $\epsilon' = \epsilon/2$, giving $y_\epsilon = 1$. It is more meaningful, however, to retain all orders of ϵ . If we iterate the RG until $\epsilon' \sim \epsilon_s$, where ϵ_s is some sufficiently small value of the renormalized coupling ϵ' , we find the corresponding value of the rescaling parameter: $b \sim (\epsilon_s/\epsilon)^{1/y_\epsilon}$. Since this occurs as a consequence of rescaling space by a factor of b^{-1} , we infer the crossover length $L_{xo} \sim (\epsilon_s/\epsilon)^{1/y_\epsilon}$. On lengthscales $\ell \gg L_{xo}$ we thus expect hierarchical, sub-diffusive relaxation. We plot this crossover length in Figure 5, and find that for $\epsilon_s = 10^{-3}$ we obtain good agreement with the phenomenological crossover length $a(c, \epsilon)$. Note that since ϵ_s is arbitrary we require additional physical input to fix the absolute scale of the crossover length. The predicted trend of increasing L_{xo} with increasing ϵ , however, is illuminating.

As an aside, and a further demonstration of the predictive power of the RG scheme, it is interesting to note that a real-space RG calculation suggests a 'bifurcation' at

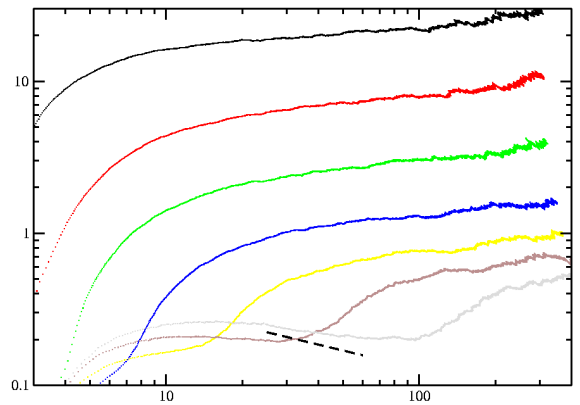


FIG. 6: Top: Real-space RG prediction for the dynamic exponent z for an attractive FA model as a function of attraction strength ϵ ; $c = 10^{-3}$. Note the bifurcation for $\epsilon \gtrsim 8$. Bottom: A test of the RG calculation – Elapsed time rescaled by the square of the mean domain length τL^{-2} versus mean domain length L for $c = 10^{-3}$ and $\epsilon = 0, 2, 4, 6, 8, 10, 12$ (top to bottom). We show averages over 5 runs for each attraction strength, starting from initial excitation concentration $n(0) = \frac{1}{2}$. For the topmost curves the scaling prediction $\tau \sim L^2$, for which $\tau L^{-2} \sim \text{const.}$, is reasonably demonstrated. For $\epsilon > 8$ (the two lowest curves) we see a regime in which $\tau \sim L^z$ with $z < 2$, as predicted by the RG calculation. We show as a heavy black dashed line the prediction $\tau \sim L^{1.60}$ for $\epsilon = 12$.

large ϵ of the dynamic exponent for an attractive version of the FA model (Figure 6, top). Our numerics support this prediction (Figure 6, bottom). Our RG treatment of the attractive FA model is a straightforward adaptation of the procedures used in Reference [18] and in this paper: we modify the embedding operator to account for the attraction ϵ , and implement the RG to first order.

VII. CONCLUSIONS

We have predicted and verified numerically that the attractive East model shows a two-stage coarsening behaviour in its out-of-equilibrium regime, as well as a non-monotonic variation of relaxation time with attraction strength. In doing so, we have shown that the real-space RG scheme of References [20, 21] successfully captures several interesting characteristics of this model, and bears out the intuitive idea of Reference [1] concerning the ‘renormalized East-like’ nature of the model at large wavelengths. Because the RG scheme may be motivated in simple physical terms, it is therefore a useful starting point in directing more detailed analyses, either numerical or theoretical.

The two-stage coarsening mechanism of the attractive East model is an example of two-stage relaxation induced by a competition between a static attraction and a kinetic constraint. It would be interesting to search for such a mechanism in real systems. The attractive East model was intended originally to be studied in its equilibrium regime, at fixed c , corresponding to fixed colloid pack-

ing fraction. To test the results of this paper against the behaviour of real attractive colloids we propose the following experiment: a sudden pressure increase at fixed T , inducing an increase in packing fraction, and hence a reduction in c as the liquid equilibrates. On the basis of our results we would expect particle mobility to differ qualitatively depending on the wavelength one probes and the isothermal compression line one explores [2]. For weak attractions and for moderate attractions at large wavelengths we would expect particle motion to be controlled principally by free volume, and thus to be sub-diffusive and repulsive glass-like. For moderate attractions at small wavelengths we would expect particles to move in an approximately diffusive manner, because attractions render the short-wavelength structure of the colloid labile.

VIII. ACKNOWLEDGEMENTS

We are grateful to YounJoon Jung, Sander Pronk and Juan P. Garrahan for discussions, and to Carlo Vandenzande for correspondance.

- [1] P.L. Geissler and D.R. Reichman, Short-ranged attractions in jammed liquids: How cooling can melt a glass, cond-mat/0402673 (2004).
- [2] K.N. Pham, S.U. Egelhaaf, P.N. Pusey and W.C.K. Poon, Phys Rev E, **59** 011503 (2004); E. Zaccarelli, F. Sciortino and P. Tartaglia, cond-mat/0406011.
- [3] G.H. Fredrickson and H.C. Andersen, Phys. Rev. Lett. **53**, 1244 (1984); J. Chem. Phys. **83**, 5822 (1985).
- [4] R.G. Palmer, D.L. Stein, E. Abrahams and P.W. Anderson, Phys. Rev. Lett. **53**, 958 (1984).
- [5] J. Jäckle and S. Eisinger, Z. Phys. **B84**, 115 (1991).
- [6] W. Kob and H.C. Andersen, Phys. Rev. E **48**, 4364 (1993).
- [7] S. Whitelam and J.P. Garrahan, J. Phys. Chem. B **108**, 6611 (2004).
- [8] M. Schulz and S. Trimper, J. Stat. Phys. **94** 173 (1999).
- [9] P. Sollich and M.R. Evans, Phys. Rev. Lett. **83**, 3238 (1999); Phys. Rev. E **68**, 031504 (2003).
- [10] A. Crisanti, F. Ritort, A. Rocco and M. Sellitto, J. Chem. Phys. **113**, 10615 (2001).
- [11] F. Chung, P. Diaconis and R. Graham, Adv. App. Math., **27**, 192, (2001).
- [12] C. Toninelli, G. Biroli and D.S. Fisher, Phys. Rev. Lett. **92**, 185504 (2004).
- [13] J.P. Garrahan and D. Chandler, Phys. Rev. Lett. **89**, 035704 (2002); Proc. Natl. Acad. Sci. USA **100**, 9710 (2003).
- [14] L. Berthier and J.P. Garrahan, J. Chem. Phys. **119**, 4367 (2003); Phys. Rev. E **68**, 041201 (2003).
- [15] F. Ritort and P. Sollich, Adv. in Phys. **52**, 219 (2003).
- [16] D.R. Reichman, E. Rabani and P.L. Geissler, Comparison of Dynamical Heterogeneity in Hard-Sphere and Attractive Glass Formers, cond-mat/0406136 (2004).
- [17] D. Chandler, *Introduction to Modern Statistical Mechanics*, Oxford University Press, New York (1987).
- [18] S. Whitelam and J.P. Garrahan, Phys. Rev. E **70**, 046129 (2004).
- [19] E.D. Siggia, Phys. Rev. B, **16**, 2319 (1977).
- [20] J. Hooyberghs and C. Vandenzande, J. Phys. A., **33**, 907, (2000); Phys. Rev. E, **63**, 041109, (2001).
- [21] A. Stella, C. Vandenzande and R. Dekeyser, Phys. Rev. B, **27**, 1812 (1983).
- [22] R.P. Feynman, *Statistical Mechanics*, Westview Press (1998).
- [23] E. Carlon, M. Henkel and U. Schollwoeck, Eur. Phys. J. B12, 99 (1999).
- [24] A. Buhot and J.P. Garrahan, Phys. Rev. E **64**, 21505 (2001).
- [25] H. Hinrichsen, Adv. Phys. **49**, 815 (2000).
- [26] J.L. Cardy, *Scaling and Renormalization in Statistical Physics*, Cambridge University Press, Cambridge (1996).
- [27] D. Aldous and P. Diaconis, J. Stat. Phys. **107**, 945 (2002).
- [28] L.P. Kadanoff, *Statistical Physics: Statics, Dynamics and Renormalization*, World Scientific Publishing (1999).